

Inclusive Distribution of Fully Reconstructed Jets in Heavy Ion Collisions at RHIC: Status Report

G. O. V. de Barros¹ for the STAR Collaboration

Instituto de Física, Universidade de São Paulo, Brazil

Abstract. We present an update to the analysis of fully reconstructed jets in heavy ion collisions by the STAR Collaboration at RHIC. We analyse the response of the anti- k_T algorithm in the presence of background, and present a new observable for the measurement of inclusive jet production that is expected to be more robust against background model assumptions than previous jet analyses at RHIC and LHC.

Keywords: Heavy Ion Collision, Full Jet Reconstruction

INTRODUCTION

The interaction of a hard-scattered parton with a colored medium, known as jet quenching, is a key probe of the Quark-Gluon Plasma (QGP) generated in high energy heavy ion collisions. In a QCD picture, jet quenching is dominated by gluon bremsstrahlung, leading to softening of the typical jet fragmentation pattern relative to jets in vacuum. The imposition of kinematic cuts on the jet constituents, including “jet” measurements via single leading hadrons, results in an apparent medium-induced energy loss of the jet, though full reconstruction of the jet should recover its full energy. Jets of finite acceptance (finite R) may nevertheless not recover the full jet energy due to large angle radiation; indeed, that is expected to be the clearest way to measure the phenomenon.

The most direct measurement of jet production and apparent energy loss due to quenching is the inclusive jet production. Such jet measurements are challenging in the complex environment of heavy ion collisions, however, due to the very large flux of soft hadrons from other, incoherent interactions in the collision. The STAR Collaboration at RHIC has previously presented the analysis of inclusive jet and hadron-jet coincidence rates in central $Au + Au$ collisions [1, 2], in which minimal kinematic cuts on the jet constituents are imposed, to achieve minimal bias of the resulting distributions. However, these analyses employed model assumptions for the influence of background on the jet measurements, and imposed kinematic cuts on the measured (i.e. jet+background) distributions themselves. Both effects need careful assessment to establish their systematic uncertainties.

In these proceedings we present a new, data-driven approach, in which the full spectrum of reconstructed jets is analysed in order to measure the fluctuations of the underlying event. We then introduce a new, differential, observable sensitive to the rate of inclusive jet production in nuclear collisions, in which the relative background contribution is substantially reduced relative to previous measurements, and indicate methods to assess the remaining background quantitatively.

DATA SAMPLE AND JET RECONSTRUCTION

This study uses $\sim 1M$ central (0 – 10%) $Au + Au$ events at $\sqrt{s_{NN}} = 200$ GeV collected by STAR during RHIC run 7. Jet reconstruction utilizes charged particles measured in the Time Projection Chamber (TPC) and neutral energy measured in the Barrel Electromagnetic Calorimeter (BEMC) [3]. All tracks and towers with $p_T > 0.2$ GeV/c are used as input for the jet reconstruction. Jets are reconstructed by k_T [4] and anti- k_T [5] algorithms with resolution parameter $R = 0.4$ using an energy recombination scheme, as implemented in FASTJET [6]. The anti- k_T algorithm is used to reconstruct signal jets and the k_T algorithm to evaluate the median background energy density. A jet is accepted if its centroid lies within $|\eta| < 0.6$.

¹ gbarros@dfn.if.usp.br

Because of the complex interplay between the hard jet component (high Q^2) and fluctuations in measured jet energy due to the underlying event, in this analysis we define a “jet” operationally, simply as the direct output of the reconstruction algorithm. We relegate the separation of hard jet and background to a separate step. The “Direct” jet transverse energy is defined as [7]:

$$p_T^{\text{direct}} = p_T^{\text{reco}} - \rho \cdot A_{\text{reco jet}}, \quad (1)$$

where p_T^{reco} is the reconstructed jet transverse energy (anti- k_T), $A_{\text{reco jet}}$ is its area [8], and $\rho = \text{median} \left\{ p_T^{\text{reco},i} / A_{\text{reco jet},i} \right\}$ is the event-wise median energy density evaluated with k_T algorithm [7]. Therefore, p_T^{direct} is corrected on an event-wise basis for the overall level of background, but not for its region-to-region fluctuations.

In this study we consider only jets with $A_{\text{reco jet}} > 0.4sr$, which is efficient for hard jets in large background but biases against jets comprising soft background only [9].

ANALYSIS AND RESULTS

Jet quenching corresponds to the medium-induced modification of jet fragmentation, and robust reconstruction of quenched jets should have minimal sensitivity to details of the fragmentation. In order to quantify the sensitivity of anti- k_T reconstruction to fragmentation in the presence of large background, we embed simulated jets with known structure into real STAR central $Au + Au$ events, apply jet reconstruction to the hybrid events, identify the reconstructed jet containing the embedded objection, and calculate [9]:

$$\delta p_T = p_T^{\text{reco}} - \rho \cdot A_{\text{reco jet}} - p_T^{\text{embed}}, \quad (2)$$

where p_T^{embed} is the embedded transverse energy.

We have explored a variety of jet fragmentation patterns and jet energies: single pions, and jets generated at $\sqrt{s} = 200$ GeV via PYTHIA (p+p) and QPYTHIA (“p+p quenched”) [10]. Figure 1, left panel, shows the response δp_T^π for single 30 GeV pions averaged over 8M different STAR central events [9]. To look in more detail, the specific sensitivity to fragmentation is isolated by comparing δp_T event-wise for two different fragmentation patterns embedded into the same event. Figure 1, right panel, shows the distribution in event-wise difference

$$\Delta \delta p_T = \delta p_T^\pi - \delta p_T^{\text{jet}}, \quad (3)$$

between δp_T for a PYTHIA-generated jet with $p_T > 30$ GeV (“probe”) and that for a single pion with the same p_T, η, ϕ . The distribution is calculated using 1M different PYTHIA jets/single pions in different STAR events. With high probability ($\sim 73\%$ in this case), the response of anti- k_T is within 200 MeV the same for two very different fragmentation patterns. Similar results are obtained for much lower jet p_T , and for QPYTHIA-generated quenched jets. This quantifies the *insensitivity* of anti- k_T to the fragmentation pattern in the presence of a heavy-ion background event, a crucial property for jet quenching studies. Anti- k_T appears to respond geometrically [5].

Figure 2, left panel, shows the Direct jet energy distribution (eq. (1)) for two different centrality classes: 0 – 5% and 5 – 10%. Due to the operational definition in this analysis of a jet simply as the output of the jet reconstruction corrected event-wise for median background level, a large fraction of the “jets” in the distribution have apparently unphysical negative energy. This is trivially due to the fact that ρ is the median energy density. However, we expect the negative energy “jets” to be dominated by combinatorial jets arising from incoherent soft processes, and will use their distribution to constrain our estimate of background fluctuations. In addition, the hard jet component lies on top of the fluctuations and is broadly distributed in the figure; imposing any cut on p_T^{direct} introduces an arbitrary threshold whose effect is difficult to quantify.

The centrality classes in Figure 2, left panel, differ in average charged particle multiplicity by $\sim 12\%$. In contrast, we find that the reconstructed jet multiplicity in the acceptance for $A_{\text{reco jet}} > 0.4sr$ differs between the two classes by less than $\sim 0.3\%$. We have found that this approximate invariance of jet multiplicity persists over at least a factor two variation in charged multiplicity. This again indicates that the response of anti- k_T is dominantly geometric: the number of jets in the acceptance is to a large extent constant, while the Direct energy distribution varies as the relative hard and combinatorial components of the event change.

This observation suggests that the hard jet component might be best isolated by observing the *evolution* of the Direct jet spectrum with change in event structure, specifically with change in centrality. Figure 2, right panel, shows

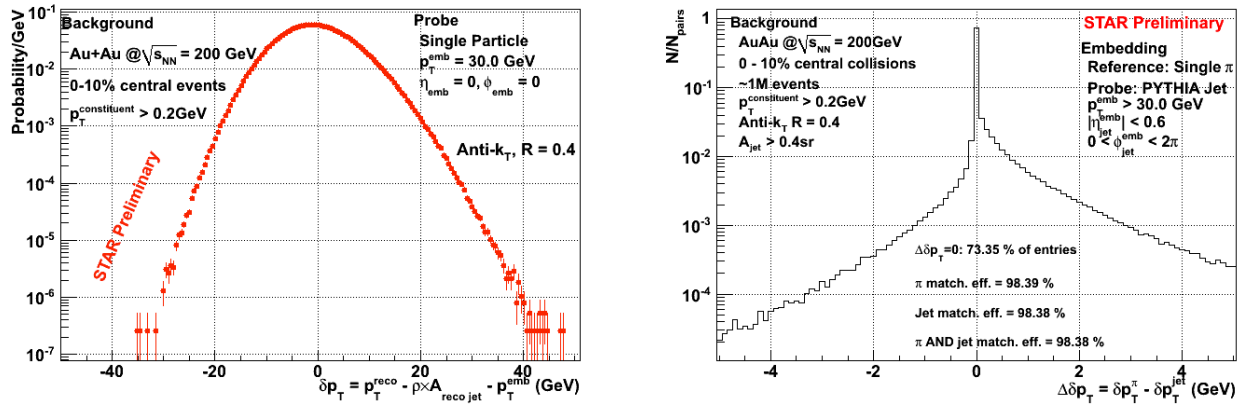


FIGURE 1. Left: response of jet reconstruction for a single pion embedded with $p_T = 30$ GeV. Right: event-wise comparison of response (eq. (2)) to a PYTHIA embedded jet ($p_T > 30$ GeV) and a single pion with same kinematics.

the *difference* between the two distributions in the left panel, illustrating the redistribution of Direct jet energy with change in centrality: for more central events there is an enhancement in both background ($p_T^{\text{direct}} \lesssim -10$ GeV) and signal ($p_T^{\text{direct}} \gtrsim 10$ GeV) regions. The dip about zero is another manifestation of the observed conservation of total jet multiplicity.

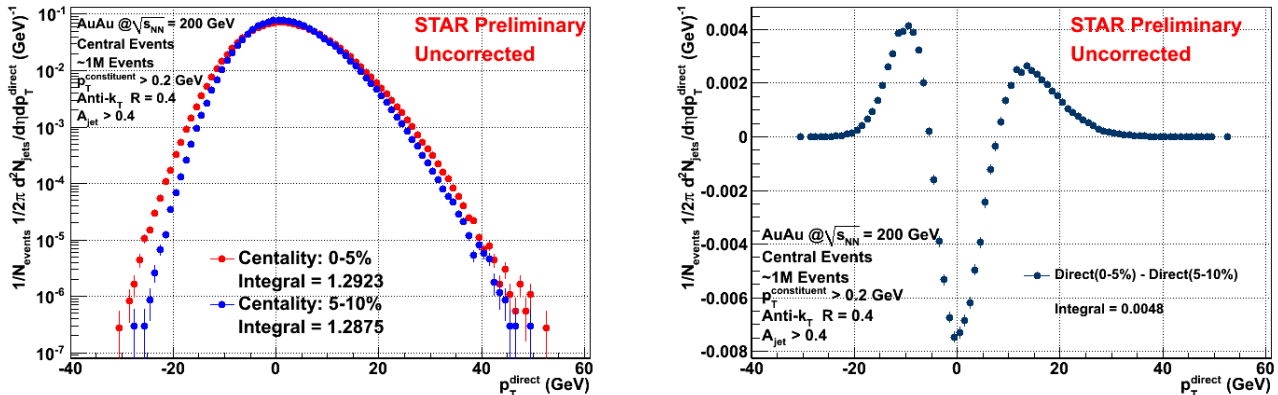


FIGURE 2. (Color online) Left: Direct jet spectra for two different event centralities: 0 – 5% (red) and 5 – 10% (blue). Right: difference between the two spectra.

We now utilize the region $p_T^{\text{direct}} < 0$ to give a data-driven estimate of the combinatorial (background) jet distribution, by fitting a Gamma function in the negative region and extrapolating to the positive region. This functional form for the distribution of transverse energy in a finite acceptance corresponds to the independent emission of a large number of particles drawn from an exponential p_T distribution [11]. A related function has been found to describe the distribution of a closely related observable, event-wise mean p_T ($\langle p_T \rangle$) at the SPS [12] and RHIC [13, 14]. The distribution has contributions from multiple sources of fluctuations, both few-particle and global, such as reaction plane orientation and residual dependence on event centrality. The Gamma-fn. parametrization includes all such effects with proper averaging.

Figure 3, left panel, shows the Gamma-fn. fit to the negative region, and extrapolation to the positive region, for the Direct jet spectrum for 0 – 5% central events. The fit describes the negative region well over $\sim 3 - 4$ orders of magnitude. The right panel compares the difference between the fits for different centralities to that for the data (same as Fig. 2, right panel). As expected, there is a good agreement between the data and the fit in the negative region of the difference spectrum. The fit difference overshoots the data difference at moderate $p_T^{\text{direct}} > 0$ while undershooting it for $p_T^{\text{direct}} \gtrsim 10$ GeV. This is expected, since the growth at large p_T^{direct} for more central collisions is due in part to

additional hard jets, which must displace a fraction of soft jets in order to conserve total jet number.

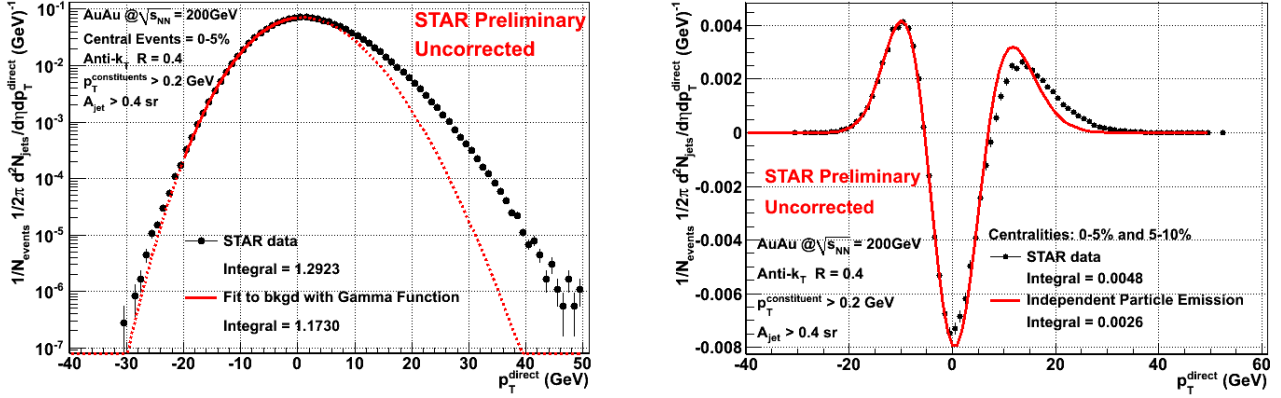


FIGURE 3. Direct jet spectrum for 0 – 5%, fitting and extrapolation (left panel) and difference spectrum and difference between fitted functions (right panel).

OUTLOOK

The final analysis of the hard jet component is beyond the scope of these proceedings. Further systematic investigation of background corrections, that are independent of the Gamma-function ansatz, are in progress. Alternative functional forms for the background estimation are also under investigation. However, we note that an important check on the hard component to be extracted from Fig. 3, right panel, comes from the well-established binary-collision scaling of hard process rates in nuclear collisions. Glauber modeling indicates that $\langle N_{bin} \rangle \sim 1000$ for the 0-5% centrality class, while $\langle N_{bin} \rangle \sim 800$ for 5-10%. Thus, difference spectrum in Fig. 2 must reflect the jet production rate due to ~ 200 additional binary collisions. Implicit, of course, is the assumption that quenching effects do not vary significantly between the centrality bins.

REFERENCES

1. S. Salur for the STAR Collaboration, *Eur. Phys. J.* **61**, 761–767 (2009).
2. M. Ploskon for the STAR Collaboration, *Nucl. Phys.* **A830**, 255c–258c (2009).
3. B. I. Abelev, et al., *Phys. Rev. Lett.* **97**, 252001 (2006), hep-ex/0608030.
4. S. Catani, Y. L. Dokshitzer, M. H. Seymour, and B. R. Webber, *Nucl. Phys.* **B406**, 187–224 (1993).
5. M. Cacciari, G. P. Salam, and G. Soyez, *JHEP* **04**, 63 (2008).
6. M. Cacciari, G. P. Salam, and G. Soyez, *FastJet 2.4.4 user manual* (2010), URL {<http://fastjet.fr/>}.
7. M. Cacciari, and G. P. Salam, *Phys. Lett.* **B659**, 119–126 (2008).
8. M. Cacciari, G. P. Salam, and G. Soyez, *arXiv:0802.1188v2 [hep-ph]* (2008).
9. P. M. Jacobs, *arXiv:1012.2406v2 [nucl-ex]* (2010).
10. N. Armesto, L. Cunqueiro, and C. A. Salgado, *arXiv:0907.1014 [hep-ph]* (2009).
11. M. J. Tannenbaum, *Phys. Lett.* **B498**, 29–34 (2001).
12. H. Appelshauser et al., *Phys. Lett.* **B459**, 679–686 (1999).
13. J. Adams et al. (STAR Collaboration), *Phys. Rev.* **C71**, 064906 (2005).
14. J. Adams et al. (STAR Collaboration), *Phys. Rev.* **C72**, 044902 (2005).